Synaptopodin and 4 novel genes identified in primary sensory neurons

Nathalie Verpoorten,[a] Kristien Verhoeven,[a] Stefan Weckx,[a] An Jacobs,[a] Sally Serneels,[a] Jurgen Del Favero,[a] Chantal Ceuterick,[c] Dirk R. Van Bockstaele,[d] Zwi N. Berneman,[d] Ludo Van Den Bosch,[e] Wim Robberecht,[e] Lucilla Nobbio,[f] Angelo Schenone,[f] Eric Dessaud,[g] Odile deLapeyrière,[g] Danny Huylebroeck,[h] An Zwijsen,[h] Peter De Jonghe,[a,b] and Vincent Timmerman[a,*]

[a]*Peripheral Neuropathy Group, Department of Molecular Genetics, Flanders Interuniversity Institute for Biotechnology (VIB), Institute Born-Bunge, University of Antwerp, Universiteitsplein 1, B-2610 Antwerpen, Belgium*
[b]*Division of Neurology, University Hospital of Antwerp, Antwerpen, Belgium*
[c]*Laboratory of Neuropathology and Electronmicroscopy, Institute Born-Bunge, University of Antwerp, Antwerpen, Belgium*
[d]*Laboratory of Experimental Hematology, University of Antwerp, University Hospital of Antwerp, Antwerpen, Belgium*
[e]*Laboratory for Neurobiology, Department of Experimental Neurology, University of Leuven, Leuven, Belgium*
[f]*Department of Neurological and Vision Sciences, University of Genova, Genova, Italy*
[g]*INSERM U.623, Developmental Biology Institute of Marseille, (CNRS, INSERM, Université de la Méditerranée), Marseille, France*
[h]*Department of Developmental Biology, VIB, Laboratory of Molecular Biology (Celgen), University of Leuven, Leuven, Belgium*

We performed differential gene expression profiling in the peripheral nervous system by comparing the transcriptome of sensory neurons with the transcriptome of lower motor neurons. Using suppression subtractive cDNA hybridization, we identified 5 anonymous transcripts with a predominant expression in sensory neurons. We determined the gene structures and predicted the functional protein domains. The *4930579P15Rik* gene encodes for a novel inhibitor of protein phosphatase-1 and *9030217H17Rik* was found to be the mouse gene *synaptopodin*. We performed in situ hybridization for all genes in mouse embryos, and found expression predominantly in the primary class of sensory neurons. Expression of *4930579P15Rik* and *synaptopodin* was restricted to craniospinal sensory ganglia. Neither *synaptopodin*, nor any known family member of *4930579P15Rik*, has ever been described in sensory neurons. The identification of protein domains and expression patterns allows further functional analysis of these novel genes in relation to the development and biology of sensory neurons.

Introduction

The two major neuronal cell types of the peripheral nervous system are the sensory neurons (SN), located in the dorsal root ganglia (DRG), and the lower motor neurons (MN) in the ventral horns (VH) of the spinal cord. Peripheral SN represent a distinct functional and structural unit for processing external stimuli. They convey different modalities of sensory information that are selectively or predominantly affected in diseases such as hereditary sensory neuropathies (HSN) (Auer-Grumbach, 2004). On the other hand, MN are selectively degenerated in hereditary motor neuropathies (HMN) (Irobi et al., 2004). Although the primary gene defect is known for some of these disorders, the selective involvement remains enigmatic. The identification of genes specifically expressed in SN will help to identify critical pathways that can explain their selective vulnerability in HSN.

Differential expression studies in the sensory part of the peripheral nervous system allow to determine gene expression profiles in this tissue and cell types therein (Newton et al., 2000; Xiao et al., 2002; Cameron et al., 2003; Araki et al., 2001). One such study has explored the differential gene expression between large- and small-sized SN using microarrays (Luo et al., 1999). A recent study illustrated that, in microarrays, 20 to 30% of the transcripts that can be identified by SSH are not identified in microarray studies because these transcripts are novel or underrepresented on the chip (Cao et al., 2004). Recently, suppression subtractive hybridization (SSH) was successfully applied to identify genes involved in normal sensory neurogenesis (Nelson et al., 2004). We also performed differential gene expression profiling by SSH to compare the transcriptome of SN isolated from DRG with the transcriptome of lower MN, which form the motor counterpart of the peripheral nerves, to identify genes specifically expressed in SN.

Here, we report the identification of 5 transcripts that represent novel genes. In situ hybridization in mouse embryos at different stages of gestation revealed that these 5 genes are predominantly expressed in craniospinal sensory ganglia.

Results

Purification of sensory and motor neurons

Differential expression profiling in the nervous system is generally complicated by the coexistence of many different cell types. Therefore, we purified SN and MN from their respective tissues to compare the expression profiles of distinct neuronal populations without confounding contamination by other cell types. By automatic counting during flow cytometric cell sorting (FCCS), a mean of 48 DRG (one embryo) provided 376,000 cells. The highly enriched population of SN (population 1, Fig. S1A, supplementary data) contained 162,000 cells or 43% of the initial cell population. The percentage of dead cells obtained by the ethidium bromide (EB) assay was 6% (population 3, Fig. S1B, supplementary data). After FCCS, the population of dead cells in the enriched SN cell population increased to almost 45% (data not shown). In consistence with flow cytometric cell viability analysis, immunocytochemistry (ICC) of the SN demonstrated a lot of death cell fragments (arrows on Fig. S2B, supplementary data). Despite the high cellular death, we decided to use this technique because the resulting population of intact cells was a very pure population of sensory neurons (Fig. S2B, supplementary data). As large cells are more vulnerable than small cells, we assume that our purified SN cell population contained almost no large proprioceptive neurons and a lot of small nociceptive and thermoceptive neurons. Two VH (one embryo) provided 555,000 cells whereas the MN-enriched population counted 125,000 cells. This represented 22% of the original cell population. This was consistent with the representation of purified MN cells from rat VH tissue, reported by Camu and Henderson (1992, 1994).

Subtracted SN-cDNA library

We constructed a cDNA library enriched for SN-specific transcripts by subtracting MN cDNA from SN cDNA. We obtained 429 differentially expressed clones that yielded 56 unique contigs. These contigs represented 32 known genes, 14 partial cDNA clones, and 10 contigs with only homology to genomic sequences in public databases. To confirm the differential expression of the 32 genes and 3 randomly selected partial cDNA clones, virtual Northern blot hybridization (cDNA blotting) and multiplex reverse transcriptase PCR (RT-PCR) was performed. Differential expression was confirmed by both methods for 15 of the 32 genes and 1 of the 3 partial cDNA clones (Table 1). Four of the 15 genes identified in the SN-cDNA library were previously reported to be differentially expressed in SN: the transient receptor potential cation channel subfamily V member 1, *Trpv1*, the voltage-gated sodium channel type IX alpha, *Scn9a*, advillin and contactin 2 (Caterina et al., 1997; Toledo-Aral et al., 1997; Shibata et al., 2004; Perrin et al., 2001). Trpv1 is a nociceptor-specific vanilloid receptor that is activated by, e.g., noxious heat stimuli. The identification of this gene in our SN library fits with our selective enrichment of nociceptive and thermoceptive neurons. The identification of known SN-specific genes underscores the specificity of the SN subtraction cDNA library. Interestingly, we identified 4 novel genes (*4930579P15Rik*, *A530088H08Rik*,

Table 1
Genes identified in the subtracted SN-cDNA library and confirmed to be differentially expressed

Mouse SN-genes	Human gene symbol	Human accession number	Virtual NB		Multiplex RT-PCR	
			MN	SN	VH	DRG
Known genes						
matrilin 2	*MATN2*	NM_002380	–	++	32c	26c
contactin 2	*CNTN2*	NM_005076	–	++	26c	23c
sodium channel, voltage-gated, type IX, alpha	*SCN9A*	NM_002977	+	+++	29c	23c
trancient receptor potential cation channel, subfamily V, member 1	*TRPV1*	NM_018727	–	+++	>	29c
pituitary tumor-transforming 1 interacting protein	*PTTG1IP*	NM_004339	–/+	++	26c	23c
fibroblast growth factor 13	*FGF13*	NM_004114	–	++	>	23c
diacylglycerol kinase, eta	*DGKH*	NM_152910	–	++	29c	26c
advillin	*AVIL*	NM_006576	–	++	32c	23c
echinoderm microtubule-associated protein like 1	*EML1*	NM_004434	–/+	++	26c	23c
epimorphin	*EPIM*	NM_001980	–	+	29c	23c
dysferlin	*DYSF*	NM_003494	–/+	+++	29c	23c
AK020250 (Hs: Synaptopodin)	*SYNPO*	NM_007286	–	+++	>	23c
Unknown genes						
2310005P05Rik (Hs: KIAA1706)	*KIAA1706*	NM_030636	–	++	29c	23c
4930579P15Rik (Hs: LOC151242)	*LOC151242*	XM_087137	–	++	29c	23c
A530088H08Rik (Hs: gene located on chr. 17)	–	–	–/+	+++	32c	23c
D130067I03Rik (Hs: KIAA1679)	*KIAA1679*	XM_046570	–	+++	29c	23c

For each gene, the mouse gene name and human gene symbol and accession number (NCBI, August 2004) are provided. For some mouse genes, no human orthologue was found in the public databases (Hs: –). Hybridization signals obtained for MN and SN by virtual Northern blotting were interpreted as: very strong (+++), strong (++), present (+), weak (–/+), or absent (–). Multiplex RT-PCR results are summarized by number of PCR cycles (ranging from 23 to 32 cycles) when a PCR product was first observed in VH or DRG. The symbol > is used when no PCR product was observed after 32 cycles.
MN: motor neuron; SN: sensory neuron; VH: ventral horn; DRG: dorsal root ganglia; c: cycles.

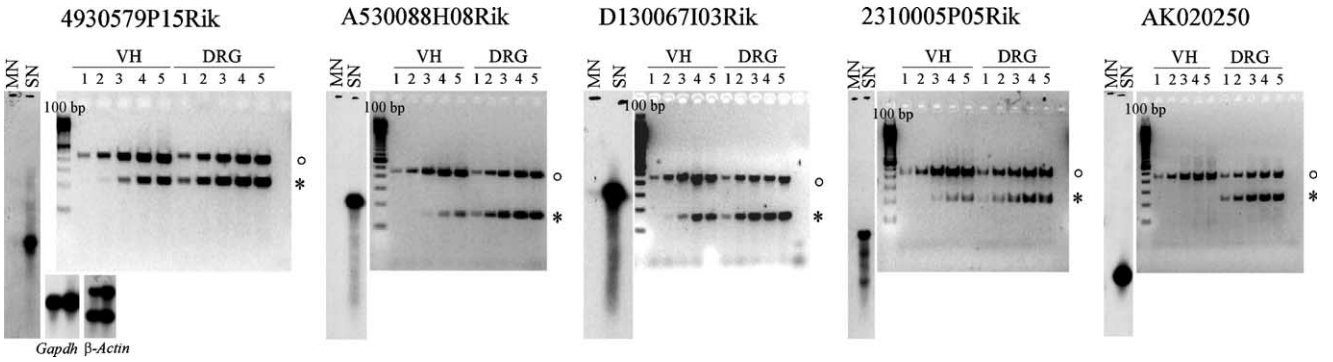

Fig. 1. Virtual Northern blots showing the differential expression of the transcripts in a MN- and SN-enriched cDNA population. The blots were also hybridized with *Gapdh* and *β-actin* as a control for the amount of cDNA loaded. Multiplex RT-PCR shows the differential expression of the transcripts in a VH- and DRG-cDNA population. *Gapdh* (°) was amplified together with the "gene-of-interest" (*) for 5 different PCR cycle sets (lanes 1–5; 23, 26, 29, 32, and 35 cycles, respectively).

D130067I03Rik, *2310005P05Rik*) and 1 cDNA clone (AK020250), which were confirmed as being differentially expressed by all methods used (Fig. 1).

Characteristics of 5 unknown genes

In order to characterize the gene structure of the 5 differentially expressed transcripts, *4930579P15Rik*, *A530088H08Rik*, *D130067I03Rik*, *2310005P05Rik*, and AK020250, we performed rapid amplification of cDNA ends (RACE) and applied different bio-informatics tools to determine known protein domains and motifs. *4930579P15Rik* (NM_172420, NP_766008), localized on mouse chromosome 2, was recently identified as a new regulatory subunit of protein phosphatase-1 (PP1), *Ppp1r1c*, based upon the presence of a protein phosphatase inhibitor-1 or DARPP-32 domain (NCBI, August 2004). The ORF spans only 327 bp, spread over 5 coding exons (Fig. 2). Ppp1r1c is significantly shorter than Ppp1r1a and Ppp1r1b, two other members of this PP1 inhibitor subfamily. Sequence homology between 4930579P15Rik and Ppp1r1a/Ppp1r1b is restricted to the N-terminal region, containing all structural elements for PP1 binding and inhibition, including the RVXF-type motif necessary for binding to PP1 (aa 7–11), and the phosphothreonine to inhibit PP1 activity (aa 34) (Fig. 2) (Wakula et al., 2003).

The second transcript, *A530088H08Rik* (NM_178656, NP_848771), maps to mouse chromosome 11 and has two exons of which only one is coding (Fig. 2). By RACE, we extended the 3′ UTR of *A530088H08Rik* (AL645988, 46229–47405) and identified a polyA signal (-AATAAA-) 18 bp upstream of the new polyA tail. In this gene, only 9.53% of the sequence is coding. No human orthologue for *A530088H08Rik* is present in the NCBI databases. However, a homology search in the public databases revealed more than 80% homology with a sequence on human chromosome 17p13.3 (NT_010718.15, 10.326.329–10.325.887). The human

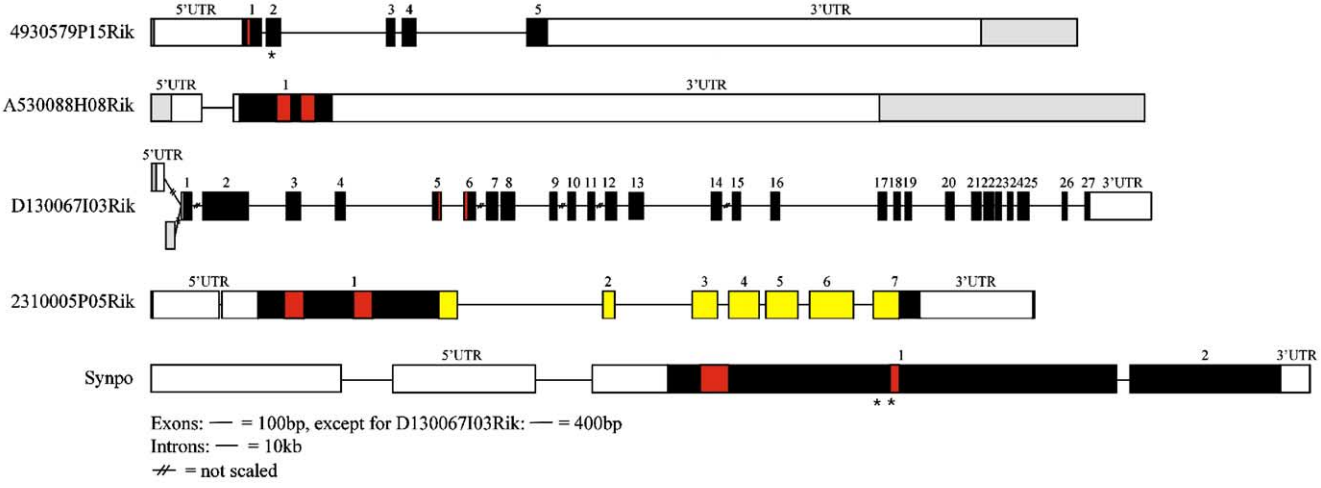

Fig. 2. Genomic organization of 4 novel genes and *Synpo*. The genomic organization of each gene is based upon the sequence data retrieved from the mouse genome (August 2004) and was confirmed by sequence analysis upon PCR. The coding exons are represented by black boxes, introns by lines and 5′ and 3′ untranslated regions (UTR) by white boxes. Gray boxes are additional UTR sequences identified by RACE. All splice events follow the GT/AG rule. For *4930579P15Rik*, the RVXF-binding motif (red box) as well as the phosphorylation site necessary for inhibition of PP1 (*) are marked. For *A530088H08Rik*, both TMH domains (red boxes) are indicated. *D130067I03Rik* is displayed with both possible 5′ UTR exons and its cytochrome b/b_6 domain (red boxes). The TSR domains are spread over the whole gene. For *2310005P05Rik*, both helix–hairpin–helix motifs (red boxes) and the endonuclease/exonuclease/phosphatase domain (yellow boxes) are shown. The gene structure of *Synpo* is deduced from homology to the rat and human orthologue and confirmed by sequencing. *Synpo* contains 2 PEST region (red boxes) and 2 PPXY motifs (*). The 7 PXXP motifs are spread over the whole gene.

putative translation initiation codon (at position 10.326.305) is consistent with the Kozak consensus sequence (ACG**ATG**G), and splicing follows the GT/AG rule. Rat and chicken orthologues map to chromosomes 10 and 18, respectively, and have a similar genomic structure. TMPred, PSORT II, and PredictProtein (PHDhtm) confirmed the presence of 2 predicted transmembrane helices (TMH) in the C-terminal part of the protein as predicted by Ensemble (Fig. 2).

The third transcript, *D130067I03Rik* (NM_172485, NP_766073), a large gene of 4824 bp spread over 27 exons, maps to chromosome 1 in the mouse (Fig. 2). The gene contains one non-coding exon in the 5′ UTR of the reference sequence. Approximately 50% of our clones, obtained through 5′-RACE, identified an additional 90 bases upstream from the non-coding exon, whereas the other clones did not contain the known non-coding exon. Instead, another non-coding exon of 158 nucleotides was identified (Fig. 2). By genomic alignment, the novel exon followed the canonical GT–AG rule. The human orthologue of *D130067I03Rik* is *KIAA1679*, located on chromosome 2. InterPro identified between 10 and 15 'thrombospondin type 1 repeat' domains (TSR) depending on the search method (Pfam, Smart, ProSite). SignalP predicted a signal peptide with cleavage site at amino acids 31–32 which indicates a secretory property. Using MGI, InterPro, and PredictProtein, we detected an N-terminal cytochrome b/b_6 heme in KIAA1679 (Fig. 2). Cytochrome b/b_6 constitutes an integral membrane protein that functions in the respiratory chain complex III of mitochondria. MitoProt indeed predicts a probability of 86% for export to mitochondria. Psort II also identified a cleavage site for mitochondrial precursor proteins at amino acids 19–20, which supports the mitochondrial involvement of D130067I03Rik.

The fourth transcript, *2310005P05Rik*, localizes on mouse chromosome 9. The human orthologue is *KIAA1706* on chromosome 7p14. It consists of one 5′ non-coding exon and 7 coding exons. This gene contains 2 helix–hairpin–helix motifs at the N-terminal segment and an exonuclease/endonuclease/phosphatase domain near the C-terminal end, predicting a DNA-binding ontology (Fig. 2). It shows no clear homology to any other known gene or protein. Additionally, none of the nuclease/phosphatase proteins contain one or more helix–hairpin–helix motifs. PredictNLS could not identify a nuclear localization signal, but PSORT II predicted a nuclear location with a nuclear localization signal at amino acids 321–327.

Finally, we identified a sequence in the cDNA library that was part of the partial cDNA clone, AK020250 (AK020250: 241–659). AK020250 has recently been updated by XM_488855 resulting in a predicted gene, *9030217H17Rik* (NCBI update August 2004). This predicted gene is located on mouse chromosome 18 and consists of 2 exons. We were unable to amplify and sequence the first 136 bp, representing the first coding exon of *9030217H17Rik*. By PCR and sequencing, we could link our sequence (contained in AK020250) with the coding region of the gene *synaptopodin* (*Synpo*), the first known gene upstream. This implicates that AK020250 is likely the 5′ UTR of *Synpo* and that *9030217H17Rik* is probably artificial. As no reference sequence for mouse *Synpo* is available in the NCBI databases, we characterized the mouse gene based on homology to the rat and human orthologue and confirmed it by direct sequencing. This resulted in an ORF of 2073 bp as reported by Mundel et al. (1997). The coding sequence of *Synpo* is within one exon while the identified 5′ UTR region is spread over 2 untranslated exons (Fig. 2). *Synpo* codes for synaptopodin, a very basic protein with no significant homology to any known protein, except for its recently discovered homologue myopodin. Due to its high content of proline (~13%) uniformly distributed over the protein, formation of any globular domain is impossible. Multiple PXXP motifs are identified throughout the protein as well as 2 PPXY motifs. PXXP motifs serve as potential SH3 domain binding sites, whereas PPXY motifs mediate the interaction with the WW domain of a variety of structural and signal transduction proteins (Kay et al., 2000). Additionally, 2 PEST motifs have been identified (Weins et al., 2001). These PEST motifs, together with the high proline content, render Synpo very susceptible for rapid degradation by the proteasome (Rechsteiner and Rogers, 1996).

Markers for craniospinal ganglia

We subsequently performed whole-mount in situ hybridization (ISH) in midgestation mouse embryos (E9.5, E10.5, E12.5) to investigate the spatial and temporal expression domains of the 5 genes during DRG development. None of the transcripts could be detected at E9.5 by whole-mount ISH (data not shown). At E10.5, we detected hybridization signals for *4930579P15Rik*, *D130067I03Rik*, and *2310005P05Rik* (Figs. 3A, B). At E12.5, *4930579P15Rik*, *A530088H08Rik*, and *D130067I03Rik* showed high expression in DRG while *Synpo* was only weakly expressed (Fig. 3C). For *2310005P05Rik*, no clear expression pattern could be detected at E12.5.

To obtain more details on the expression domains of the genes, sagittal and transverse sections of E13.5 mouse embryos were hybridized with radioactively labeled antisense probes for each gene. As expected, all genes – including *Synpo* – were strongly expressed in DRG (Fig. 4A). Additionally, all transcripts showed high expression levels in almost all cranial sensory ganglia (Figs. 4B, C). The cranial ganglia include the trigeminal (V), facial (VII), vestibulocochlear (VIII), glossopharyngeal (IX), and vagal (X) ganglia, located lateral to the hindbrain (Cordes, 2001). Cranial nerves I and II, respectively, the olfactory and optic nerve, are pure sensory nerves but do not have sensory ganglia. Instead, their cell bodies are located in the sense organs, the olfactory epithelium and the ganglionic layer of the retina, respectively. In the olfactory epithelium, only *D130067I03Rik* was expressed, although *Synpo* was very weakly expressed in the precartilage primordium of the nasal capsule and septum (data not shown). The retina of E13.5 mouse embryos does not yet consist of the characteristic layers present in adult retina and is called neuroretina. The ganglion cells, located in the sensory layer of E13 retina, expressed all analyzed genes, except *2310005P05Rik* (Fig. 5). Instead, the *2310005P05Rik* transcript was present in the lens epithelium and cornea (Fig. 5). Expression in sensory nuclei in the hindbrain was also detected for *4930579P15Rik*, *A5300088H08Rik*, and *2310005P05Rik* (data not shown).

Gene expression analysis at the level of the spinal cord (Fig. 6) again confirmed the difference in expression of all genes in SN as compared to MN. MN are topographically organized in the spinal cord (Jessell, 2000; Pfaff and Kintner, 1998). Somatic MN are subdivided into 2 discrete columns, the medial motor column (MMC) and the lateral motor column (LMC) that, in turn, are subdivided into medial and lateral compartments and that are located at distinct positions within the axial and rostrocaudal planes of the spinal cord. MN within each column innervate a specific set

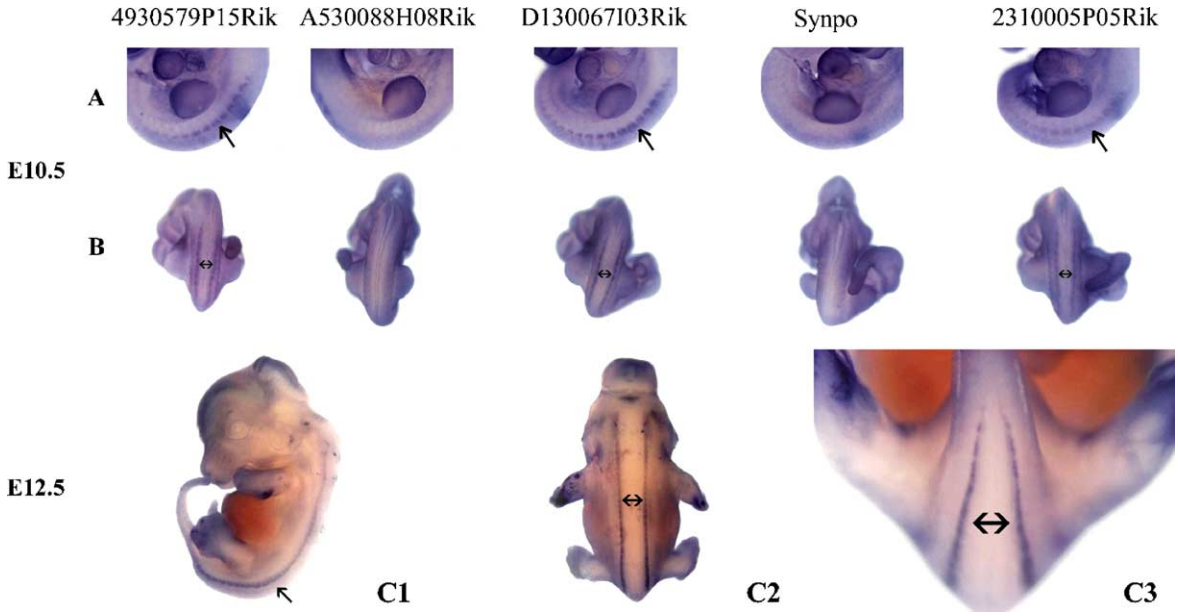

Fig. 3. Whole-mount in situ hybridization reveals expression of the SN-specific genes in DRG. Lateral (A) and dorsal (B) views of E10.5 embryos illustrate the expression of *4930579P15Rik*, *D130067I03Rik*, and *2310005P05Rik* in DRG (arrows), whereas no expression can be detected in DRG for *A530088H08Rik* and *Synpo*. A lateral (C1), dorsal (C2), and high-power caudal (C3) view at E12.5 show high expression in DRG for *D130067I03Rik* (arrows). *4930579P15Rik* and *A530088H08Rik* revealed the same expression pattern and a similar but weaker expression is observed for *Synpo* (data not shown). No distinct expression pattern was observed for *2310005P05Rik* (data not shown).

of skeletal muscles; those within the MMC innervate axial and body wall muscles, while MN within the LMC innervate limb musculature. Only a weak expression of *4930579P15Rik* and *A5300088H08Rik* was found in the spinal cord, in particular in the LMC located at brachial and lumbar levels, as compared to expression in SN (Fig. 6A). Weak expression for *D130067I03Rik* was observed along the spinal cord in the MMC (Fig. 6A), while the spinal cord was completely devoid of *Synpo* and *2310005P05Rik* (Fig. 6B). These expression patterns were confirmed by whole-mount ISH on isolated spinal cords of E13.5

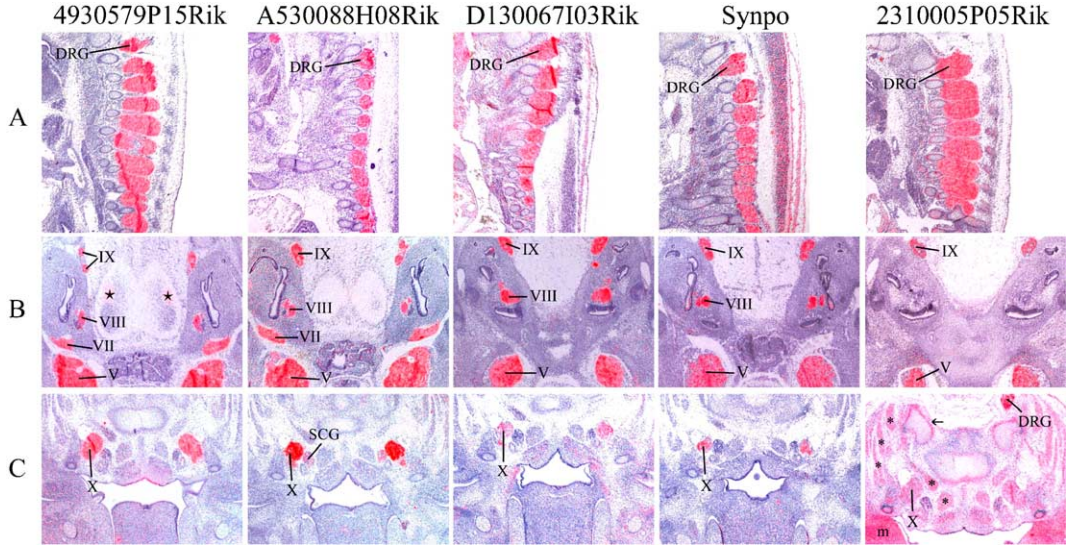

Fig. 4. Radioactive ISH was performed on sections of E13.5 mouse embryos. Sagittal sections (A) show expression of all 5 genes in DRG. A more detailed expression pattern is shown in the transverse sections (B and C). Most other primary SN, localized in cranial sensory ganglia, show expression of these genes. *4930579P15Rik*, *A530088H08Rik*, and *D130067I03Rik* are strongly expressed in all cranial ganglia, including the trigeminal (V), facial (VII), vestibulocochlear (VIII), glossopharyngeal (inferior and superior IX), and vagal (inferior and superior X) ganglia. Expression of *D130067I03Rik* and *2310005P05Rik* in VII is not seen on the slide shown in this picture. High expression of *Synpo* could be detected in all cranial ganglia except in VII. *2310005P05Rik* is expressed in all cranial ganglia except in VIII. Additional expression domains were identified: a distinct nucleus in the pons shows weak expression of 4930565M23Rik (★), and *A5300088H08Rik* is weakly present in superior cervical ganglia (SCG) containing sympathetic neurons. The ISH for *2310005P05Rik* revealed a broad expression pattern for this gene (C). Although *2310005P05Rik* expression in DRG is much stronger, it is also present in muscles (*), around cartilage structures (←), and in the mesenchyme between oropharyngeal cavity and ear entrance (m).

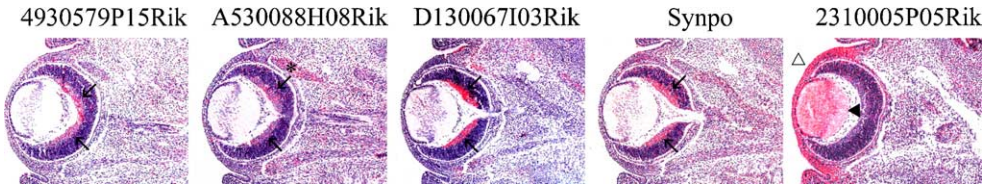

Fig. 5. Expression analysis of novel SN-genes in the eye. The optic nerve contains no sensory ganglia; instead, the sensory neurons are located in the ganglionic layer of the retina. Expression in the ganglion cells is detected for all genes (←), except for *2310005P05Rik*, which is expressed in the lens epithelium (◀) and the cornea (◁). *A5300088H08Rik* is also expressed in the eye musculature (*).

mouse embryos (Fig. 6A). Additionally, these experiments revealed *A5300088H08Rik* expression in the floor plate of the spinal cord (Fig. 6A). The signal of *A5300088H08Rik* in the floor plate as well as in the lumbar MN was only very weakly detected by radioactive ISH on transversal sections. The colocalization of the mRNA of *4930579P15Rik*, *A5300088H08Rik*, or *D130067I03Rik* in Islet1/2 protein positive cells, further supports the presence of these genes in postmitotic somatic MN (data not shown). Additional colocalization experiments are necessary to identify the distinct MN pools that express these genes.

For *A5300088H08Rik*, *D130067I03Rik*, and *2310005P05Rik*, additional, though significantly weaker, expression domains were observed and listed in Table A (Supplementary data). For *A5300088H08Rik*, we detected weak expression in cervical and thoracic sympathetic neurons (Figs. 4C and 6A, respectively) and in a distinct layer of the stomach and duodenum, possibly representing the sympathetic innervation of these organs (data not shown).

To document the expression of these genes in DRG beyond midgestation, we analyzed their expression at postnatal day 0 (P0). Expression of *4930579P15Rik*, *A5300088H08Rik*, and *2310005P05Rik* is maintained in brachial, thoracal, and lumbar postnatal DRG (Fig. 7). Yet, expression is not homogeneous throughout the ganglion. Expression of *Synpo* and *D130067I03Rik* is not detected in postnatal DRG (data not shown).

Discussion

Vertebrate sensory neurons form a distinct functional and structural unit in charge of processing external stimuli. Given their role as conveyors for different modalities of sensory information, it is crucial to understand the molecular mechanisms that regulate the development and maintenance of sensory neurons. According to anatomical location, sensory ganglia can be further divided into cranial ganglia and dorsal root ganglia.

In this paper we report the identification of *Synpo* and 4 novel SN-genes by comparing the transcriptome of SN with that of MN. Differences in the transcriptome of both cell types can result from cell-type-specific gene expression but also from different timing in neuronal birth and subsequent development since SN develop at a later stage than MN. On the other hand, different subpopulations of SN and MN also develop according to different time courses and according to a rostrocaudal gradient (Kitao et al., 2002; Hollyday

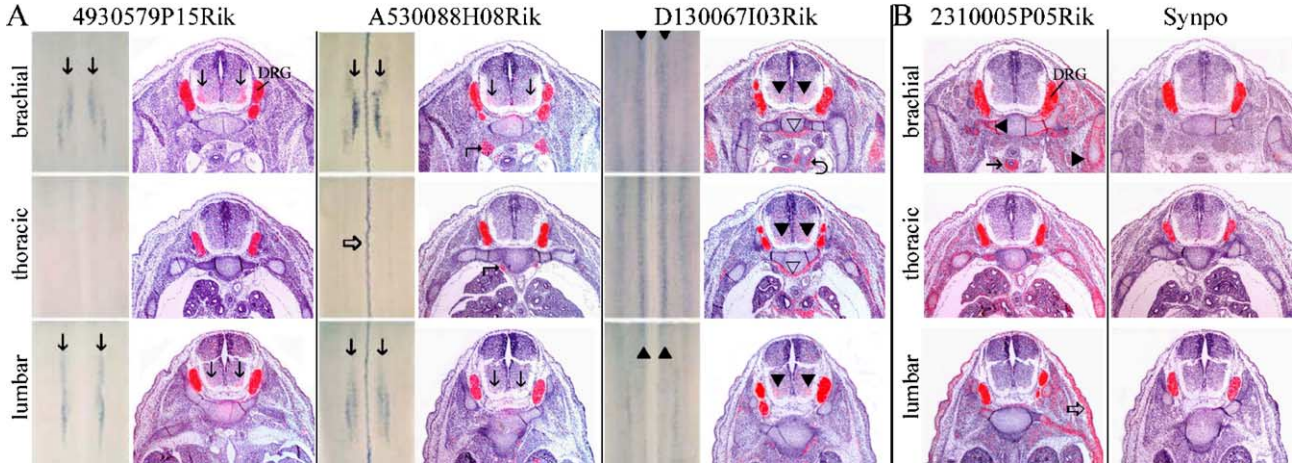

Fig. 6. Expression analysis in the spinal cord. (A) Whole-mount ISH on isolated spinal cord (left panels) and radioactive ISH on transversal sections of the spinal cord at the brachial, thoracic, and lumbar level (right panels) of E13.5 embryos. On the transversal sections, *4930579P15Rik*, *A5300088H08Rik*, and *D130067I03Rik* are expressed in MN but the hybridization signal is substantially weaker than in SN of DRG. *4930579P15Rik* and *A5300088H08Rik* are only expressed by MN at the brachial and lumbar level, representing the lateral motor column (↓). These MN innervate the muscles of the limbs. A weak expression of *D130067I03Rik* is observed all along the spinal cord in the medial motor column (▼). These 3 expression patterns are confirmed by whole-mount ISH on isolated spinal cords of E13.5 mouse embryos. Additional expression of *A5300088H08Rik* is detected in the floor plate (⇨). The signal of *A5300088H08Rik* in the floor plate as well as in the lumbar MN is only very weakly detected by radioactive ISH on transversal sections. Panel B shows ISH of transversal sections for *Synpo* and *2310005P05Rik* at the level of the spinal cord. No hybridization signal is obtained in the spinal cord. The slides (A and B) also show expression of *A5300088H08Rik* in thoracic sympathetic ganglia (↱), located more ventral to the vertebra, expression of *2310005P05Rik* around cartilage structures (▶ and ◀), as also around trachea (→) and in surface ectoderm (⇨), and expression of *D130067I03Rik* in mesenchyme ventral from vertebra (▽) and around the ductus arteriosus (⮌) is observed.

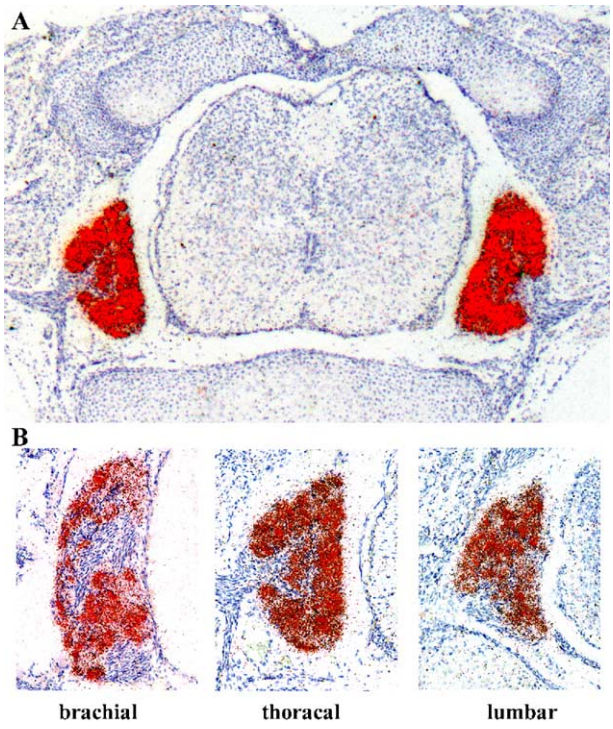

Fig. 7. Radioactive ISH was performed on transverse sections of P0 mice. An overall picture of the expression of *A5300088H08Rik* at the level of the thoracal spinal cord is shown in panel A with enlargement of a DRG at the brachial, thoracal, and lumbar level (B). *4930579P15Rik* and *2310005P05Rik* revealed the same expression pattern, but no expression was observed in DRG for *Synpo* and *D130067I03Rik* (data not shown).

and Hamburger, 1977). On top of that, cell sorting has altered the subpopulation composition of DRG neurons, enriching for small nociceptive neurons, and changes in the transcript profile could have occurred during the isolation procedure. Despite all these, the 5 novel transcripts identified here showed remarkable uniform expression in all DRG neurons along the rostrocaudal axis at midgestation in wild type E13.5 mouse embryos. Expression analysis of these transcripts in P0 DRG is indicative of a more restricted expression within the DRG. Likewise, the expression in DRG of Cntn2, another gene identified in our SN cDNA library, becomes restricted to one subpopulation of SN (Perrin et al., 2001). Co-expression studies will be required to identify the different SN-subtypes unequivocally.

The most restricted expression pattern was observed for *Synpo*. Synaptopodin is an actin-associated protein specifically localized in dendritic spines of telencephalic adult neurons, as well as in differentiated renal podocyte foot processes (Mundel et al., 1997). Podocytes and neurons share many features, such as their process formation and highly organized cytoskeletal systems (Kobayashi, 2002). The well-documented association of *Synpo* with both actin and the spine apparatus renders *Synpo* crucial for process motility. Additionally, dendritic spine formation and remodeling are involved in synaptic plasticity that represents the morphological basis of long-term memory (Yamazaki et al., 2001). Synaptopodin-deficient mice lack the spine apparatus and show deficits in synaptic plasticity and learning (Deller et al., 2003). *Synpo* is reported to be expressed postnatally in distinct regions of the brain and in differentiating podocytes, but not in SN. In the adult brain, expression of *Synpo* is detected only in the olfactory bulb, cerebral cortex, striatum, and hippocampus, representing regions of high synaptic plasticity. In this study, we described the embryonic expression pattern of the *AK020250* transcript that represents the 5′ UTR of *Synpo*. The messenger was exclusively detected in primary SN, located in craniospinal ganglia at midgestation. Expression was however absent at P0. These novel embryonal expression domains of *Synpo* shed new light on its function, as well as on SN development and synapse formation.

The *4930579P15Rik* transcript is also restricted to the nervous system with high expression in primary SN and weaker expression in LMC-MN. The gene belongs to the *IPP1* and *DARPP-32* subfamily. IPP1 and DARPP-32 are phosphoproteins that inhibit phosphatase activity of PP1 (Shenolikar, 1995). *PP1* is ubiquitously expressed and regulatory subunits, including its endogenous inhibitors, control subcellular localization and substrate specificity of PP1. The inhibitor *IPP1* is widely expressed in mammalian tissues, whereas *DARPP-32* is predominantly expressed in the nervous system, more specifically in dopaminoceptive neurons (Joutel et al., 1996). Here, *Ppp1r1c* expression is very restricted. The identification of a novel endogenous inhibitor of *PP1* with high and selective expression in primary SN is indicative of a tight regulation of PP1's phosphatase activity in neuronal cell growth and differentiation.

The *2310005P05Rik*, *A5300088H08Rik*, and *D130067I03Rik* transcripts have a more widespread expression pattern. The expression pattern of *2310005P05Rik* at E10.5 indicates that it becomes first expressed in SN. The widespread expression in, e.g., muscles detected at E13.5, possibly masks the DRG-expression pattern in whole-mount E12.5 embryos. Interestingly, *A5300088H08Rik* is expressed in the floor plate. The floor plate is an important signaling center composed of non-neuronal cells that controls neuronal differentiation. It also secretes guidance molecules that direct navigating axons crucial for correct wiring of neuronal circuits (Strahle et al., 2004). The absence of functional protein domains hampers suggestions on functional roles for *A530088H08Rik*. The large *D130067I03Rik* transcript contains several TSR repeats. These repeats are found in extracellular matrix proteins such as F-spondin. F-spondin is a cell adhesion molecule that promotes neurite outgrowth and the attachment of spinal cord cells and sensory neurons (Klar et al., 1992). The expression of *D130067I03Rik* in SN and in spinal cord, in addition to the presence of TSR repeats and a signal peptide, might suggest a similar function. On the other hand, the presence of an N-terminal cytochrome b/b_6 domain in *D130067I03Rik*, an N-terminal cleavage site for mitochondrial precursor proteins, and the high prediction of transport to mitochondria suggest mitochondrial involvement.

The identification of novel genes in the peripheral nervous system suggests still unknown biological mechanisms that can be relevant for the biology of primary sensory neurons. In addition, novel genes identified during SN development might point to genes that are also implicated in disease, like, for example, nerve growth factor (Lewin and Mendell, 1993). Hence, all our 5 genes are putative new candidates for peripheral sensory neuropathies, although none of these genes so far map to a locus currently known for inherited sensory neuropathies (Auer-Grumbach, 2004).

In conclusion, we have used SSH as a method to detect known – and most importantly – also novel genes expressed in peripheral sensory neurons. The 5 genes analyzed in this study revealed a predominant expression in primary sensory neurons with

two of these (*4930579P15Rik* and *Synpo*) showing a very restricted expression pattern. The identification of protein domains and expression patterns provides a starting point for future functional analysis of these genes to elucidate their function and to provide new insights into sensory neuron development and biology.

Experimental methods

Animals

All experiments were performed on NMRI mice (IFFA CREDO, Les Oncins, France), a normal mouse strain. Embryos were obtained by cesarean section. The day of the vaginal plug was considered as embryonic day 0 (E0). The Ethical Committee for Animal Experiments, University of Antwerp, Belgium approved the study.

cDNA library construction

From E13.5, we isolated DRG from all cranio-caudal levels and ventral horns as described by Johnson and Bunge (1992) and Juurlink (2003), respectively. Purification of SN from DRG single cell suspensions was performed using FCCS (FACSVantage SE, BD, San Jose, California) (Salzman et al., 1990; Carter and Ormerod, 2000). Forward- (FSC) and side scatter (SSC) signals were visualized on a density plot to obtain an informative pattern of the whole DRG single cell population using WinMDI version 2.8 software (Windows Multiple Document Interface for Flow Cytometry, http://www.facs.scripps.edu/software.html) (Fig. S1, supplementary data). The density plot resulted in three groups of cells of different size with the largest one (population 1 in Fig. S1A, supplementary data) sorted out by an electric field and counted automatically. The percentage of dead cells was calculated with an EB assay (Fig. S1B, supplementary data) (St John et al., 1986). To evaluate the effect of the flow cytometric sorting of the cell population, the same EB assay was performed on the sorted population of neurons. For the purification of MN from ventral horn single cell suspension, we used a 6.4% metrizamide (Sigma, St. Louis, Missouri) cushion as previously described (Schnaar and Schaffner, 1981; Vandenberghe et al., 1998). The quality of the SN and MN cell suspensions was analyzed by ICC before and after isolation by FCCS or the metrizamide gradient (Fig. S2, supplementary data).

We extracted total cellular RNA from purified SN and MN cell populations using the Totally RNA™ Kit (Ambion, Austin, Texas) and treated it with RNase-free DNase I (DNA-free™, Ambion). One microgram of the total RNA was used to synthesize cDNA using the SMART PCR cDNA Synthesis Kit (Clontech, Palo Alto, California). We optimized the number of PCR cycles to 17. This cDNA then served as a template for SSH (Diatchenko et al., 1999). The PCR-Select cDNA Subtraction Kit (Clontech) for SSH was used according to the manufacturer's protocol using SN-cDNA as 'tester' and MN-cDNA as 'driver', adding the following modifications: 30 cycles of the primary suppression PCR and 11 cycles of the secondary nested PCR was carried out at 67°C annealing temperature with the Advantage cDNA polymerase mix (Clontech).

We purified subtracted cDNA with the NucleoTrap Nucleic Acid Purification Kit (Clontech) and 10 ng cDNA was inserted into the T/A cloning vector pT-Adv (Clontech). After electroporation in DH5α *E. coli* (Life Technologies, San Diego, California), 4460 colonies were picked. To identify true differentially expressed clones on a high-throughput basis, we used the PCR-Select Differential Screening Kit (Clontech) to make colony arrays in duplo and hybridize these with 3 different ^{32}P-labeled cDNA pools, the subtracted SN-cDNA pool and both unsubtracted SN- and MN-cDNA populations. A total of 429 differentially expressed colonies were selected for sequence analysis.

Sequence analysis and annotation

We sequenced all 429 cDNA clones using the DYEnamic ET Terminator Cycle Sequencing kit (Amersham). Sequence reactions were run on an ABI PRISM™ 3700 DNA Analyzer (Applied Biosystems, Foster City, California) and analyzed by SSHSuite (Weckx et al., 2004). In summary, the quality of the sequences was checked with Phred (Ewing et al., 1998; Ewing and Green, 1998), retaining 399 sequences for further analysis. The 399 sequences were masked for vector and adaptor sequences using CrossMatch and assembled in 72 contigs using Phrap (http://www.phrap.org/). The contigs were compared with the information available in the public databases (Genbank) using NCBI-BLAST (http://www.ncbi.nlm.nih.gov/BLAST/).

Virtual Northern blot analysis

One microgram of the original, but unsubtracted, cDNA from SN and MN neuronal cell populations was denatured, electrophoresed overnight on 1% Seakem agarose (FMC BioProducts, Rockland, Maine)/TAE (Life Technologies) gels, and blotted on Hybond-XL membranes (Amersham). We amplified the 32 genes and 3 of the partial cDNA clones using M13 universal primers. The PCR products were radioactively labeled, and hybridized on the cDNA blots. Equal loading of cDNA was confirmed by rehybridization with two housekeeping genes *Gapdh* and *β-actin*.

Multiplex RT-PCR

One microgram of total RNA from 'unpurified' whole DRG and VH tissue was reverse-transcribed using Superscript™ First-Strand Synthesis System for RT-PCR (Life Technologies) with oligo-dT primers. The cDNA then served as template for PCR amplification using two pairs of primers, one for housekeeping gene *Gapdh*, serving as an internal control, and one for a specific gene or partial cDNA clone from the cDNA libraries. We designed primers as such to allow discrimination between the *Gapdh* fragment of 451 bp and the PCR product of the gene-of-interest on a 2% agarose (Life Technologies)/TBE (Sigma) gel. In order to retrieve semi-quantifiable PCR results, different numbers of PCR cycles (23–26–29–32–35 cycles) were performed to follow the amplification of the *Gapdh* and the "gene-of-interest" transcripts in both neuronal tissues.

Gene structure analysis

To deduce the full-length transcripts of 5 unknown transcripts, we performed 5′ and 3′ RACE using GeneRacer™ (Life Technologies) and sequencing analysis. In search of possible homologues and orthologues of the resulting full-length transcripts, we submitted these to the Genbank database (http://www.ncbi.nlm.nih.gov) and Ensemble (http://www.ensemble.org). In order to

retrieve extra information on putative domains and motifs, we explored InterPro (http://www.ebi.ac.uk/interpro/), MGI (Mouse Genome Information, http://www.informatics.jax.org/), TMPred (http://www.ch.embnet.org/software/TMPRED_form.html), PSORT II (http://www.psort.nibb.ac.jp/form2.html), PredictNLS (http://www.cubic.bioc.columbia.edu/predictNLS/), MitoProt II 1.0a4 (http://www.ihg.gsf.de/ihg/mitoprot.html), and SignalP 3.0 (http://www.cbs.dtu.dk/services/SignalP/). Overall sequence analysis and structure prediction was performed using the PredictProtein server (http://www.cubic.bioc.columbia.edu/predictprotein/). The human chromosomal location was interpellated with the loci reported for inherited peripheral neuropathies (http://www.molgen.ua.ac.be/CMTMutations/).

Expression studies

In vitro transcription with T3 or T7 RNA polymerase yielded ^{35}S- or digoxigenin-labeled single-stranded antisense and sense riboprobes (*4930579P15Rik*: NM_172420, nucleotides 583–1534; *A530088H08Rik*: NM_178656, nucleotides 1535–2332; *D130067I03Rik*: NM_172485, nucleotides 1987–2796; *2310005P05Rik*: NM_026189, nucleotides 1373–2111; 5′ UTR *Synpo*: AK020250, nucleotides 241–659). Sense probes were used as negative controls (data not shown). The digoxigenin-labeled probes were used for whole-mount in situ hybridization on E9.5, E10.5, and E12.5 mouse embryos as well as on isolated E13.5 spinal cords (Wilkinson, 1992; Henrique et al., 1995). The ^{35}S-labeled riboprobes were used for ISH on 6-μm-thick paraffin sections from E13.5 embryos and P0 mice (Dewulf et al., 1995). For combined ISH/IHC, ISH was performed on 16-μm-thick frozen sections and immunostaining was carried out as described (Carroll et al., 2001).

Acknowledgments

The authors gratefully acknowledge the contribution of the VIB Genetic Service Facility (http://www.vibgeneticservicefacility.be/) in the sequencing analyses and bio-informatics support. We thank Christine Van Broeckhoven for critical reading of the manuscript. We also appreciate the help of Marc Lenjou for the cell sorting procedures and Ulla Lübke, Lisette Beek, Luk Cox, and Tom Van de Putte for histology support. This research project was supported by the Fund for Scientific Research (FWO-Flanders), the Special Research Fund of the University of Antwerp (UA) and the University of Leuven (KUL), the Medical Foundation Queen Elisabeth, the Interuniversity Attraction Poles program P5/19 and P5/35 of the Belgian Federal Science Policy Office, Belgium and the Association Française contre les Myopathies, France. The American ALS Association, USA, supports WR and LVDB. NV is supported by a PhD fellowship from the Institute for Science and Technology (IWT), KV is a postdoctoral fellow, and WR a clinical investigator of the FWO-Flanders, Belgium. ED is supported by a PhD fellowship from the Fondation pour la Recherche Médicale, France.

Appendix A. Supplementary data

References

Araki, T., Nagarajan, R., Milbrandt, J., 2001. Identification of genes induced in peripheral nerve after injury. Expression profiling and novel gene discovery. J. Biol. Chem. 276, 34131–34141.

Auer-Grumbach, M., 2004. Hereditary sensory neuropathies. Drugs Today 40, 385–394.

Cameron, A.A., Vansant, G., Wu, W., Carlo, D.J., Ill, C.R., 2003. Identification of reciprocally regulated gene modules in regenerating dorsal root ganglion neurons and activated peripheral or central nervous system glia. J. Cell. Biochem. 88, 970–985.

Camu, W., Henderson, C.E., 1992. Purification of embryonic rat motoneurons by panning on a monoclonal antibody to the low-affinity NGF receptor. J. Neurosci. Methods 44, 59–70.

Camu, W., Henderson, C.E., 1994. Rapid purification of embryonic rat motoneurons: an in vitro model for studying MND/ALS pathogenesis. J. Neurol. Sci. 124, 73–74.

Cao, W., Epstein, C., Liu, H., DeLoughery, C., Ge, N., Lin, J., Diao, R., Cao, H., Long, F., Zhang, X., et al., 2004. Comparing gene discovery from Affymetrix GeneChip microarrays and Clontech PCR-select cDNA subtraction: a case study. BMC. Genomics 5, 26.

Carroll, P., Gayet, O., Feuillet, C., Kallenbach, S., De Bovis, B., Dudley, K., Alonso, S., 2001. Juxtaposition of CNR protocadherins and reelin expression in the developing spinal cord. Mol. Cell. Neurosci. 17, 611–623.

Carter, N.P., Ormerod, M.G., 2000. Introduction to the principles of flow cytometry. In: Ormerod, M.G. (Ed.), Flow Cytometry: A Practical Approach. Oxford Univ. Press, Oxford, pp. 1–22.

Caterina, M.J., Schumacher, M.A., Tominaga, M., Rosen, T.A., Levine, J.D., Julius, D., 1997. The capsaicin receptor: a heat-activated ion channel in the pain pathway. Nature 389, 816–824.

Cordes, S.P., 2001. Molecular genetics of cranial nerve development in mouse. Nat. Rev. Neurosci. 2, 611–623.

Deller, T., Korte, M., Chabanis, S., Drakew, A., Schwegler, H., Stefani, G.G., Zuniga, A., Schwarz, K., Bonhoeffer, T., Zeller, R., et al., 2003. Synaptopodin-deficient mice lack a spine apparatus and show deficits in synaptic plasticity. Proc. Natl. Acad. Sci. U. S. A. 100, 10494–10499.

Dewulf, N., Verschueren, K., Lonnoy, O., Moren, A., Grimsby, S., Van de Spiegle, K., Miyazono, K., Huylebroeck, D., Ten Dijke, P., 1995. Distinct spatial and temporal expression patterns of two type I receptors for bone morphogenetic proteins during mouse embryogenesis. Endocrinology 136, 2652–2663.

Diatchenko, L., Lukyanov, S., Lau, Y.F., Siebert, P.D., 1999. Suppression subtractive hybridization: a versatile method for identifying differentially expressed genes. Methods Enzymol. 303, 349–380.

Ewing, B., Green, P., 1998. Base-calling of automated sequencer traces using phred: II. Error probabilities. Genome Res. 8, 186–194.

Ewing, B., Hillier, L., Wendl, M.C., Green, P., 1998. Base-calling of automated sequencer traces using phred: I. Accuracy assessment. Genome Res. 8, 175–185.

Henrique, D., Adam, J., Myat, A., Chitnis, A., Lewis, J., Ish-Horowicz, D., 1995. Expression of a Delta homologue in prospective neurons in the chick. Nature 375, 787–790.

Hollyday, M., Hamburger, V., 1977. An autoradiographic study of the formation of the lateral motor column in the chick embryo. Brain Res. 132, 197–208.

Irobi, J., De Jonghe, P., Timmerman, V., 2004. Molecular genetics of distal hereditary motor neuropathies. Hum. Mol. Genet. 13, 195–202.

Jessell, T.M., 2000. Neuronal specification in the spinal cord: inductive signals and transcriptional codes. Nat. Rev., Genet. 1, 20–29.

Johnson, M.I., Bunge, R.P., 1992. Primary cell cultures of peripheral and central neurons and glia. In: Fedoroff, S., Richardson, A. (Eds.), Protocols for Neuronal Cell Culture. The Human Press Inc., pp. 13–38.

Joutel, A., Corpechot, C., Ducros, A., Vahedi, K., Chabriat, H., Mouton, P., Alamowitch, S., Domenga, V., Cecillion, M., Marechal, E., et al., 1996. Notch3 mutations in CADASIL, a hereditary adult-onset condition causing stroke and dementia. Nature 383, 707–710.

Juurlink, B.H.J., 2003. Chick spinal somatic motoneurons in culture. In: Fedoroff, S., Richardson, A. (Eds.), Protocols for Neuronal Cell Culture. The Human Press Inc., pp. 39–51.

Kay, B.K., Williamson, M.P., Sudol, M., 2000. The importance of being proline: the interaction of proline-rich motifs in signaling proteins with their cognate domains. FASEB J. 14, 231–241.

Kitao, Y., Robertson, B., Kudo, M., Grant, G., 2002. Proliferation patterns of dorsal root ganglion neurons of cutaneous, muscle and visceral nerves in the rat. J. Neurocytol. 31, 765–776.

Klar, A., Baldassare, M., Jessell, T.M., 1992. F-spondin: a gene expressed at high levels in the floor plate encodes a secreted protein that promotes neural cell adhesion and neurite extension. Cell 69, 95–110.

Kobayashi, N., 2002. Mechanism of the process formation; podocytes vs. neurons. Microsc. Res. Tech. 57, 217–223.

Lewin, G.R., Mendell, L.M., 1993. Nerve growth factor and nociception. Trends Neurosci. 16, 353–359.

Luo, L., Salunga, R.C., Guo, H., Bittner, A., Joy, K.C., Galindo, J.E., Xiao, H., Rogers, K.E., Wan, J.S., Jackson, M.R., et al., 1999. Gene expression profiles of laser-captured adjacent neuronal subtypes. Nat. Med. 5, 117–122.

Mundel, P., Heid, H.W., Mundel, T.M., Kruger, M., Reiser, J., Kriz, W., 1997. Synaptopodin: an actin-associated protein in telencephalic dendrites and renal podocytes. J. Cell Biol. 139, 193–204.

Nelson, B.R., Sadhu, M., Kasemeier, J.C., Anderson, L.W., Lefcort, F., 2004. Identification of genes regulating sensory neuron genesis and differentiation in the avian dorsal root ganglia. Dev. Dyn. 229, 618–629.

Newton, R.A., Bingham, S., Davey, P.D., Medhurst, A.D., Piercy, V., Raval, P., Parsons, A.A., Sanger, G.J., Case, C.P., Lawson, S.N., 2000. Identification of differentially expressed genes in dorsal root ganglia following partial sciatic nerve injury. Neuroscience 95, 1111–1120.

Perrin, F.E., Rathjen, F.G., Stoeckli, E.T., 2001. Distinct subpopulations of sensory afferents require F11 or axonin-1 for growth to their target layers within the spinal cord of the chick. Neuron 30, 707–723.

Pfaff, S., Kintner, C., 1998. Neuronal diversification: development of motor neuron subtypes. Curr. Opin. Neurobiol. 8, 27–36.

Rechsteiner, M., Rogers, S.W., 1996. PEST sequences and regulation by proteolysis. Trends Biochem. Sci. 21, 267–271.

Salzman, G.C., Singham, S.B., Johnston, R.G., Bohren, C.F., 1990. Light scattering and cytometry. In: Melamed, M.R., Lindmo, T., Mendelsohn, M.L. (Eds.), Flow Cytometry and Sorting. John Wiley and Sons, Inc., New York, pp. 81–107.

Schnaar, R.I., Schaffner, A.E., 1981. Separation of cell types from embryonic chicken and rat spinal cord: characterization of motoneuron-enriched fractions. J. Neurosci. 1, 204–217.

Shenolikar, S., 1995. Protein phosphatase regulation by endogenous inhibitors. Semin. Cancer Biol. 6, 219–227.

Shibata, M., Ishii, J., Koizumi, H., Shibata, N., Dohmae, N., Takio, K., Adachi, H., Tsujimoto, M., Arai, H., 2004. Type F scavenger receptor SREC-I interacts with advillin, a member of the gelsolin/villin family, and induces neurite-like outgrowth. J. Biol. Chem. 279, 40084–40090.

St. John, P.A., Kell, W.M., Mazzetta, J.S., Lange, G.D., Barker, J.L., 1986. Analysis and isolation of embryonic mammalian neurons by fluorescence-activated cell sorting. J. Neurosci. 6, 1492–1512.

Strahle, U., Lam, C.S., Ertzer, R., Rastegar, S., 2004. Vertebrate floor-plate specification: variations on common themes. Trends Genet. 20, 155–162.

Toledo-Aral, J.J., Moss, B.L., He, Z.J., Koszowski, A.G., Whisenand, T., Levinson, S.R., Wolf, J.J., Silos-Santiago, I., Halegoua, S., Mandel, G., 1997. Identification of PN1, a predominant voltage-dependent sodium channel expressed principally in peripheral neurons. Proc. Natl. Acad. Sci. U. S. A. 94, 1527–1532.

Vandenberghe, W., Van Den, B.L., Robberecht, W., 1998. Glial cells potentiate kainate-induced neuronal death in a motoneuron-enriched spinal coculture system. Brain Res. 807, 1–10.

Wakula, P., Beullens, M., Ceulemans, H., Stalmans, W., Bollen, M., 2003. Degeneracy and function of the ubiquitous RVXF motif that mediates binding to protein phosphatase-1. J. Biol. Chem. 278, 18817–18823.

Weckx, S., De Rijk, P., Van Broeckhoven, C., Del Favero, J., 2004. SSHSuite: an integrated software package for analysis of large-scale suppression subtractive hybridization data. BioTechniques 36, 1043–1045.

Weins, A., Schwarz, K., Faul, C., Barisoni, L., Linke, W.A., Mundel, P., 2001. Differentiation- and stress-dependent nuclear cytoplasmic redistribution of myopodin, a novel actin-bundling protein. J. Cell Biol. 155, 393–404.

Wilkinson, D.G., 1992. Whole mount in situ hybridization of vertebrate embryos. In: Wilkinson, D.G. (Ed.), In Situ Hybridization: A Practical Approach. IRL Press, Oxford, pp. 75–84.

Xiao, H.S., Huang, Q.H., Zhang, F.X., Bao, L., Lu, Y.J., Guo, C., Yang, L., Huang, W.J., Fu, G., Xu, S.H., et al., 2002. Identification of gene expression profile of dorsal root ganglion in the rat peripheral axotomy model of neuropathic pain. Proc. Natl. Acad. Sci. U. S. A. 99, 8360–8365.

Yamazaki, M., Matsuo, R., Fukazawa, Y., Ozawa, F., Inokuchi, K., 2001. Regulated expression of an actin-associated protein, synaptopodin, during long-term potentiation. J. Neurochem. 79, 192–199.